Electrical efficiency of the heat pipe cooled photovoltaic systems

▪ **Amer Hussein Albozidi***

▪ Abstract

The solar PV modules framework has been executed into the sun oriented heat vitality utilization framework, yielding made strides sun oriented vitality use effectiveness. The two key objectives of the solar framework plan utilizing heat pipe cooling advances were the heat stream of the PV module and the exchange execution heating. Heat units (ε-NTU) approach will be utilized with regard to mechanical analysis and computation of the particular thermoelectric heat pipe efficiency. As the emerged coolant degree and plate degree, the heat and electrical yield of the unit, and the researches illustrates that the whole of distinction within the electrical and heat productivity of the framework is 6.99 percent, 7.46 percent, and 63.2 percent, respectively This article gives a promising approach to considering the proficiency of heat exchange utilizing heat pipes, which can be utilized to degree and treat the impact of factors influencing the system›s success.

Keywords: photovoltaic system, thermoelectric conversion, heat pipe cooling system.

▪ ملخص:

تناولت الدراسة كيفية تصميم الإطار الخاص بوحدات الطاقة الشمسية الكهروضوئية من خلال استخدام الطاقة الحرارية الناتجة من النظام الشمسي ،مما أدى ذلك لرفع فعالية استخدام الطاقات النظيفة المستمدة من الشمس .. الهدفان الرئيسيان لخطة إطار العمل باستخدام تبريد الأنابيب الحرارية كانا كالتالي:.

التيار الحراري للوحدة الكهروضوئية .

التسخين بالتنفيذ التبادلي .

تم استخدام نموذج الوحدات الحرارية التي تدعى (ε-NTU) طبقا للتحليل الميكانيكي وقياس كفاءة الأنابيب الكهرو حرارية طبقا لدرجة المبرد المستخدم ودرجة الشريحة المعدنية؛ يتم تقدير الناتج الحراري والكهربائي للوحدة....... تظهر الدراسة أن إجمالي التمييز في الإنتاجية الكهربائية والحرارية للإطار هو: 6.99 ٪... 7.46 ٪ .... 63.2 ٪ على الترتيب.

الدراسة تعطي مدخلا للنظر في كفاءة التبادل الحراري باستخدام الأنابيب الحرارية ، والتي يمكن استخدامها لتقدير ومعالجة تأثير العوامل التي تؤثر على نجاح تلك المنظومة.

الكلمات المفتاحية: النظام الكهروضوئي، التحول الكهرو حراري ، نظام تبريد الأنابيب الحرارية.

* **Assistant Professor Department of Mathematic Faculty of Education University of Tripoli**

Introduction

Solar PV technology, with the increasing importance of renewable energy and non-renewable energy concerns, has gained great importance for power generation [1-2]. Part of the photovoltaic energy that only matches the bandwidth can be converted into electric power by solar PV power generation techniques, but nonetheless, most thermal energy is wasted in the form of heat. Current solar cells in particular have a conversion efficiency of less than 20%, and cannot increase to 80% of photovoltaic energy to reusable energy, so there will make a significant waste of heat resulting from sunlight and on the other hand, the heat that is not used would cause the cell temperature to increase. If the temperature of the cell increases, its conversion potential decreases from 3 to 6%. [3-4]. Since Ken and Russell [5] first proposed the concept of an integrated solar photovoltaic power generation system in 1978, researchers attempted to develop cooling systems in all types of cells [6-9], and found that most cooling systems relied on forced convection cooling and natural convection cooling and found that forced cooling using water and air was the most efficient among all systems [10-14]. And native science researchers have studied solar PV technology [15-17]. It had been found that when a coolant is utilized, benefit warmth from the photo voltaic panel is going to be absorbed since it flows inside, which within turn will certainly bring about the decrease within the heat. The main reason for this is the isothermal flux denseness of photo voltaic radiation, the particular photovoltaic heating system mechanism, the particular heat circulation inside entire body, and the particular uneven submission from the coolant. (There are three types of heat transfer: conduction, radiation and convection) The specific temp degree of the photovoltaic panels must not be uniform and also, At this point, the temperature of the sunlight oriented PHOTOVOLTAIC modules should do not have to get uniform, And the working temperature of the plate should take the same path of the liquid flow and when these conditions do not exist then The cooling is asymmetric and, in some instances, "hotspots", which results in a reduction in performance of PV plate conversion, at the same time with the irregularity of the photo voltaic PV system, caused by the working temperature of the plate , makes it hard to change the working temperature With regard to solar PHOTOVOLTAIC.*et al*. [18]

System parameters

When sunlight strikes the photovoltaics' glass cover, it enters the closed space formed by the glass cover and the glass side seal of the panel, where it is absorbed by the parts of the solar cells and converted into electrical energy, then photo voltaic panels warm up, and section of the temperature will be lost via radiation plus convection. The particular heat-conducting components with outstanding thermal conductivity are transferred to the particular cell walls within the evaporation sector till it gets to the threaded heating pipe; then your operating fluid will be absorbed in to the heating pipe and subsequently evaporated, then your evaporated water flows in to the heat tube in the particular condensation field from the wick. With this field, the heating system tube operating fluid will be released in to the coolant outside the particular condensing field tube, then condenses into the liquid operating fluid. Whenever the machines are fully willing, the capillary suction actions and the particular gravitational movement from the water working liquid should go back again to the particular evaporation section of the oil wick heating tube through the particular tube in order to the adiabatic sector, after that absorb heat and escape again; Throughout chilling from the coolant, the particular liquid inlet nozzle enters the coolant inlet after which gets in to the coolant channel in to the coolant route, then the cool from the wick heat tube through the heat trade with the convection with the moisture build-up or condensation sector in the wick heat tube.

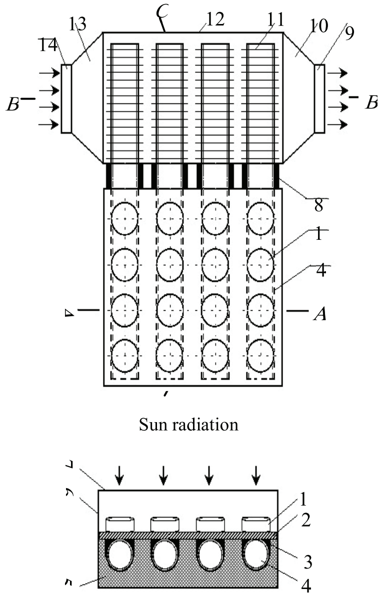

Figure 1 Sketch of hybrid thermal integrated photovoltaic

1—Solar photovoltaic module, 2—Solar photovoltaic panel, 3—Heat conducting material, 4—Heat pipe with wick, 5—Insulation material for evaporation section of wick heat pipe, 6—Glass side seal, 7—Glass cover, 8 —Insulation material for the heat pipe insulation section of the wick, 9—cooling fluid outlet pipe, 10—cooling fluid outlet header, 11—radial fin, 12—cooling fluid channel, 13—cooling fluid inlet header, 14—cooling fluid Imports take over.

Theoretical analysis:

Related assumptions

(**N** number of rows of the battery or number of heat pipes under the cell board,A_{cell} S surface area of the cell**,** ∂panel thickness, **S** solar input radiation absorbed by the solar panel,α absorption rate of solar input radiation on the panel surface, **W** the center distance between the two heat pipes, **D** the outer diameter of the heat pipe,L_e length of the evaporation section of the heat pipe, L_c length of the condensation section of the heat pipe)

Since the heat pipe is welded to the battery plate the connection area between the

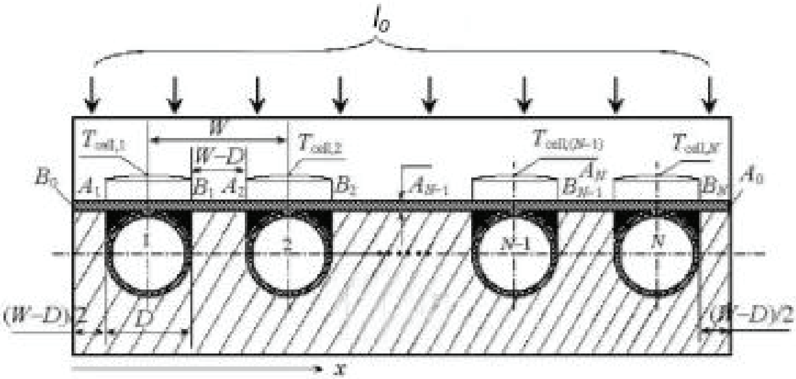

Figure 2 Explanation model for the system

heat pipe and the battery board is evenly divided int $B_1, A_2 - B_2$ $A_3 - B_3, \ldots, A_N - B_N$, their temperatures are T_{b1}、T_{b2}, T_{b3}、 … 、T_{bN} respectively .the temperature distribution of each battery column is uniform, named $T_{cell,1}, T_{cell,2}, T_{cell3,}, \ldots, T_{celln}$. Since the battery is well attached to the cell plate, it can be considered as $T_{cell1} \approx T_{b1}, T_{cell\,2} \approx T_{b2}, T_{cell3} \approx T_{b3}, \ldots, T_{celln} \approx T_{bN}$ When analyzing the temp distribution of the plate between the two heat tubes, ignoring the thermal gradient of the plate, and also assuming that the thickness of the cell plate is thin, and does not take into account the temp gradient in the direction of the thickness of the cell plate nor with the axial direction of the heat tube, you can position the plate as B_o-A_1,B_1-A_2, B_2-A_3… B_n-A_o. as Fig(1). The heat transfer problem is regarded as a typical "fin problem". This article considers the case of a glass cover with glass of region = A_o.

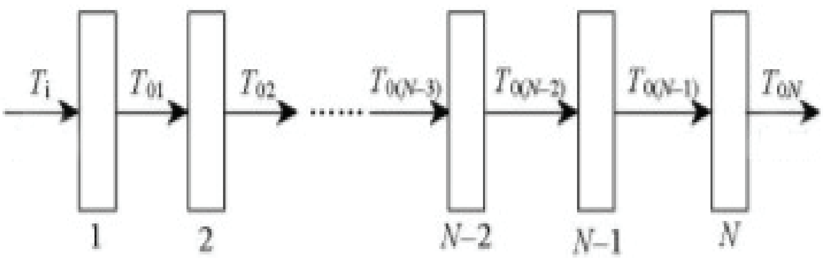

Figure 3 variation of temp of the coolant in the condensing section.

Bo-A1 region

The B_o-A_1 region of the board is thought in as a one-dimension thermal conductive with (W-D)/2 width fin. Take the solar panel micro-element body with a width of dx as showing in Fig.4. As the object, after analyzing, the heat transformation direction is being consistent with the coordination direction: Q_x is the heat being imported to the micro-element body; Q_{x+dx} the heat exportation from the micro-element body; Q_{net} is the sum of the external flow heat amount appling to this body that is measure as follows[19]:

$$q_{net} = S - U_L(T - T_a) \quad (1)$$

Where U_L = the losing heat coefficient, S is the solar panel absorption, T is the temperature and T_a is the inlet ambient temperature.

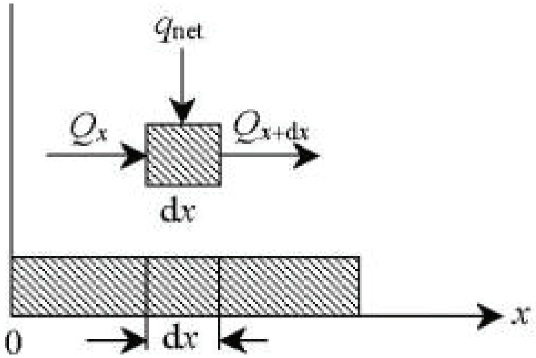

Figure 4 Element control volume of solar cell plate

The thermal conductivity differential eqn of the solar panel is obtained from the energy conservation of the micro-element body [19]:

$$\frac{d^2t}{dx^2} + \frac{S - U_L(T - T_a)}{(2)\lambda\delta} = 0 \quad (2)$$

Where λ is the thermal conductivity.

The general solution of the eqn $T = C_{0,1}\exp(mx) + C_{0,2}\exp(-mx) + (S/U_L + T_a)$ (3)

Where $m = [U_L/(\lambda\delta)]^{½}$ and $C_{0,1}, C_{0,2}$ are the integral constants , which determined by the following boundary conditions:

$$dt/dx|_{x=0} = 0 , T|_{x=(W-D)/2} = |T_{b1} \quad (4)$$

Then the temp distribution of the solar panel along the x direction is obtained as

$$T = \frac{ch(mx)}{ch(mH/2)}\left[T_{b1} - \left(\left(\frac{S}{U_L}\right) + T_s\right)\right] + \frac{S}{U_L} + T_a \tag{5}$$

The flow of heat presented at A_1 is

$$Q_{A1} = -\lambda\delta L_e \frac{dT}{dx}\Big|_{x=\frac{H}{2}} = \frac{1}{2} H L_e F[S - U_L(T_{b1} - T_a)] \tag{6}$$

where H=W–D.

The F is the efficiency of fin that can be giren by $F = [th\left(\frac{mH}{2}\right)]/\frac{mH}{2}$

Merging the general solution eqn. (3), with the heat flow introduced on node B_1 could be attained as

$$Q_{B1} = -\lambda\delta L_e \frac{dT}{dx}\Big|_{x=0} = -\lambda\delta m L_e\left(T_{b1} - 2C_{1,2} - \frac{S}{U_L} - T_a\right) \tag{7}$$

The heat flux derived at node A_2 is

$$Q_{A2} = -\lambda\delta L_e \frac{dT}{dx}\Big|_{x=W-D} = -\lambda\delta m L_e[C_{1,1}exp(mH) - C_{1,2}exp(-mH)] \tag{8}$$

The first cell of the solar radiant heat obtained in the region A_1-B_1 of the solar panel is

$$Q_{A1B1} = DL_e[S - U_L(T_{b1} - T_a)] \tag{9}$$

the first heat pipe is $Q_{hpl} = GC_p(T_{01} - T_i)$ (10)

Where Cp is the specific heat, G is the flow mass of cooling fluid, Ti is the cooling fluid inlet temp, T_{01} is the temp. of the cooling fluid after passing the condensation sector of the first pipe.

First column electric energy converted by cell [19]:

$$E_{cell,1} = \eta_{cell,1} A_{cell,1} S = A_{cell,1} I_0(\tau\alpha)\eta_{ref}\left[1 - \beta_T\left(T_{cell,1} - T_{ref}\right)\right] \tag{11}$$

In the above formula: $A_{cell,1}$ is the surface region of the cell; $\eta_{cell,1}$ is the efficiency of the photovoltaic cell; η_{ref} is the efficiency of the photovoltaic cell at the reference temp; $T_{cell,1}$ is the cell temp and Tr_{ef} is the reference temp. Taking the A_1-B_1 region of the first cell as the research object, according to the energy balance [19]:

$$|Q_{A1}| + Q_{A1B1} + |Q_{B1}| = Q_{hpl} + E_{cell,1}\ get\text{:}\ (1/2)HL_eF[S - U_L(T_{b1} - T_a)] + DL_e[S - U_L(T_{b1} - T_a)] + \lambda\delta m L_e\left(T_{b1} - 2C_{1,2} - S/U_L - T_a\right) = GC_p(T_{01} - T_i) + A_{cell,1}S\eta_{ref}\left[1 - \beta_T\left(T_{cell,1} - T_{ref}\right)\right] \tag{12}$$

The analysis of A_n-B_n region of the cell

For the A_n-B_n area of the cell in the nth (=2, 3, 4,..., N−1) column, the transfer process of heat of each area is the same. The analysis is the same as mentioned in A_1-B_1 area, and the same result is obtained [19]:

$$\lambda\delta mL_e(T_{bn}-2C_{n,2}-S/U_L-T_a)+DL_e[S-U_L(T_{bn}-T_a)]=GC_p(T_{0n}-T_{0(n-1)})+\lambda\delta mL_e[C_{n-1,1}\exp(mH)-C_{n-1,2}\exp(-mH)]+A_{\text{cell},n}S\eta_{\text{ref}}[1-\beta_T(T_{\text{cell},n}-T_{\text{ref}})] \quad (13)$$

Where:

$$C_{n-1,1}=T_{b(n-1)}-C_{(n-1),2}-(S/U_L+T_a);$$

$$C_{n-1,2}=\frac{\left[T_{b(n1)}-\left(\frac{S}{U_L}+T_a\right)\right]exp(mH)}{2sh(mH)}-\frac{\left[T_{bn}-\left(\frac{S}{U_L}+T_a\right)\right]}{2sh(mH)};$$

$$C_{n,2}=\frac{[T_{bn}-(S/U_L+T_a)]exp(mH)}{2sh(mH)}-\frac{[T_{b(n+1)}-(S/U_L+T_a)]}{2sh(mH)};$$

n□(2,3,4,5,…,N−1); $T_{b(n-1)}$ is the temp of the cell plate A_{n-1}-B_{n-1} region; T_{bn} is the temp of the cell plate A_n-B_n; $T_{b(n+1)}$ is the temp in the region A_{n+1}-B_{n+1} of the cell panel; $T_{0(n-1)}$ is the inlet temp before the cooling fluid flows through the condensation sector of the nth heat pipe; T_{0n} is the cooling fluid flows through the condensation sector of the nth heat pipe After the outlet temp.

The A_N-B_N region of the cell in column N (n=N)

B_{N-1}-A_N region to the left of the A_N-B_N region of the N^{th} heat pipe. According to the above method, the heat flow Q_{AN} derived at node A_N can be obtained; The B_N-A_0 region on the right side of the A_N-B_N (W−D)/2, where the right side of the cell plate is insulated, and the general solution is combined at this time (3) Calculate the heat Q_{BN} introduced at the node B_N as [19]

$$Q_{BN}=-\lambda\delta L_e\frac{dT}{dx}|_{x=0}=-\lambda\delta mL_e(C_{N,1}-C_{N,2}) \quad (14)$$

The region A_N-B_N vitality balance eqn of the N^{th} cell is

$$|Q_{BN}|+Q_{ANBN}=|Q_{AN}|+Q_{hpN}+E_{cell,N} \quad (15)$$

Among them, the useful heat Q_{hpN} absorbed by the cooling fluid after passing through the condensation sector of the N^{th} heat pipe is

$$Q_{hpN}=GC_p(T_{0N}-T_{0(N-1)})Q_{hpN}=GC_p(T_{0N}-T_{0(N-1)}) \quad (16)$$

Therefore, eqn (15) can be further rewritten as

$$\lambda\delta mL_e\left(2C_{N,1} - T_{bN} + S/U_L + T_a\right) + DL_e[S - U_L(T_{bN} - T_a)] = GC_p\left(T_{0N} - T_{0(N-1)}\right) + \lambda\delta mL\left[C_{N-1,1}exp(mH) - C_{N-1,2}exp(-mH)\right] + A_{cell,N}S\eta_{ref}\left[1 - \beta_T\left(T_{cell,N} - T_{ref}\right)\right] \tag{17}$$

The relationship between T_{0n} and T_{bn} for the first pipe

The heat transfer efficiency for the first heat pipe ε and the number of heat transfer units N_{TU} can be defined as:

$$\begin{cases} \varepsilon_1 = 1 - \exp(-N_{TUc1}) \\ N_{TUc1} = \left(A_{c1}U_{c,01}\right)/\left(GC_p\right) \end{cases} \tag{18}$$

Where $U_{c,01}$ is the transfer coefficient of condensing sector heat and the cooling fluid, that can be calculated using the heat transfer correlation formula $Nu = 0.26Re^{0.6}Pr^{1/3}$ of the condensing sector across the heat pipe [20] ,A_{c1} = heat pipe condensation. The coolant range is transferred from $\varepsilon_1 = (T_{01} - T_i)/\left(T_{c,01} - T_i\right)$,in $T_{c,01}$ The temperature at which the condensation sector of the pipe operates in order to provide permeability for the same temperature as the heat pipe, The high thermal coefficient of the heat pipe's inner phase transition, and the close contact between the heat pipe and the cell plate and filled with materials with outstanding thermal conductivity, it can mostly be calculated as $T_{c,01} \approx T_{b1}$ then

$$T_{01} = T_i + [1 - exp(-N_{TUc1})](T_{b1} - T_i) \tag{19}$$

For the nth (n=2, 3, 4... N) Heat pipe, there are

$$T_{0n} = T_{0(n-1)} + [1 - exp(-N_{TUcn})]\left(T_{bn} - T_{0(n-1)}\right) \tag{20}$$

And since $A_{cn} = A_{c01}, U_{c,01} = U_{c,0n}, A_{cn} = A_{c01}, U_{c,01} = U_{c,0n}$, therefore:

$$\varepsilon_1 = \varepsilon_2 = \varepsilon_3 = \varepsilon_4 = \cdots = \varepsilon_n = \varepsilon$$

Then:

$$T_{01} = T_i + \varepsilon(T_{b1} - T_i) = \varepsilon T_{b1} + (1 - \varepsilon)T_i \tag{21}$$

$$T_{02} = \varepsilon T_{b2} + (1 - \varepsilon)\varepsilon T_{b1} + (1 - \varepsilon)^2 T_i \tag{22}$$

$$T_{0n} = T_i(1-\varepsilon)^n + (1-\varepsilon)^{n-1}\varepsilon T_{b1} + (1-\varepsilon)^{n-2} \quad (23)$$

$$\varepsilon T_{b2} + \cdots + (1-\varepsilon)\varepsilon T_{b(n-1)} + \varepsilon T_{bn} \quad (24)$$

Where n∈ (2, 3, 4... N).

Obviously,accordingtotheabove T_{0n} and T_{bn} itcanbeseenfromtherelationship betweentheeqns(12),(13)and(17)thattherearexactlyNunknownsintheNeqns, and the closed solution of the eqns can be obtained, that is, the solar panel region of $A1 - B1$. The temp of $A_1 - B_1, A_2 - B_2$, $A_3 - B_3, \ldots, A_N - B_N$ and T_{b1}, T_{b2}, T_{b3}, ..., T_{bN} or the temp of the cooling fluid after passing through the condensation sector of each heat pipe are T_{01}, T_{02}, T_{03}, ..., T_{0N} T_{01}, T_{02}, T_{03}, ..., T_{0N}, which can then be The thermal efficiency of the PV-T system is obtained as

$$\eta_t = [GC_p(T_{oN} - T_i)]/(I_0 A_{coll}) \quad (25)$$

Where $A_{coll} = NWL_e$ $A_{coll} = NWL_e$. Since the battery is well attached to the cell plate, it can be considered as $T_{cell1} \approx T_{b1}, T_{cell\,2} \approx T_{b2}, T_{cell3} \approx T_{b3}, \ldots, T_{celln} \approx T_{bN}$ .Finally, the electrical efficiency of the system can be calculated is

$$\eta_e = \frac{\sum_{n=1}^{N} E_{\text{cell},n}}{I_0 A_{\text{coll}}} = \frac{\sum_{n=1}^{N} \eta_{\text{cell},n} S A_{\text{cell},n}}{I_0 A_{\text{coll}}} \quad (26)$$

Result analysis and conclusion

Figure 5 depicts a summary of the calculated outcomes and the experimental results in the literature [21] The graph shows that with 14 heat pipes and a water flow mass G = 0.0458 kg / s. Since the experimental values of the structural parameters of the solar thermal collector such as solar radiation, ambient temperature, inlet water temperature and water mass flow completely agree with the experimental conditions in the literature [21], the heat loss coefficient between the collector and the environment is UL = 8.6 W / (m2 .K) [22], the structural parameters of the photovoltaic system are: The material used is copper and the total length is 0.92 m, the length of the evaporation sector is L_e=0.75m, and the condensation sector is L_c=0.1 m, heat pipe outer diameter D=0.108m; pipe spacing W=0.135m; glass cover plate is 0.76 m×1.9 m×0.004 m; cell plate material is copper, length is 1.89 m, width is 0.75 m, cell plate coating Assuming it is an anodic aluminum oxide spectral selective absorption coating, the absorption rate is α=0.94, the transmittance of the glass cover is τ=0.9, The condensation part of the heat pipe is implanted into the cooling fluid drain. The channel length is 1.9m, and the channel sector height is 0.1 m, the width is 0.255 m, The cooling fluid traverses the condensation sector of each heat pipe in line; the number of heat pipes is N=14, and the cooling fluid is water. The number of cell rows is 14, and the coefficient of loss in heat between the cell board and environment is UL=8.6 W/ (m^2 .K) [22]. Take cell parameters η_{ref}=0.12, β_T temperature coefficient of uoc =0.0045 °C , T_{ref} the reference temp =25°C.Fig. 6 shows the change of cell temp with the number of cell rows at different times. It can be seen from Fig. 6 that the cell temp increases as the number of cell rows increases. Under the same T_i inlet water temp =37 °C , the cell temp is highest at 11 o'clock and lowest at 15 o'clock, which is consistent with the time when the outlet water temp of Fig. 6 reaches the highest and lowest. In addition, at different moments, the cell temp changes in the range that does not exceed 2.5°C, signifying that the cell's temperature has become more uniform as a result of the heat pipe's use to cool it.

Fig. 7 shows the calculation results of the electrical efficiency (solid line) and thermal efficiency (dashed line) of the PV-T system at different inlet water temps .The results revealed that as the inlet water temp increased, the PV-T system's electrical and thermal performance decreased. (Keep in mind that this is thus keeping the same level of solar radiation and atmospheric temp.). Under different inlet temps, the range of electrical efficiency changes at different moments are: 7.19%~7.46%; 7.09%~7.36%; 6.99%~7.25%. This is because as the inlet water temp increases, the cell temp also increases, and the photovoltaic power conversion efficiency of the cell decreases. Similarly, the thermal efficiency changes at different inlet temps are 59.1%~63.2%, 56.1%~59.2%, 51.0%~55.3%. The reason for this phenomenon is that as the inlet water temperature rises, so does the PV-T system's outlet water temperature, but at a slower rate than the inlet water temperature rise.

References

1. *Zheng Yingnan ,Wang Junping ,Zhang Xia .Maximum power point following control within the photovoltaic control era based on energetic identical impedance coordinating theory[J] .Proceedings of the CSEE ,2011 , 31(2):111-118*

2. *Liao Zhiling ,Ruan Xinbo .Energy administration control technique for* stand-alone photovoltaic control framework [J] .Proceedings of the CSEE ,2009 ,29(21):46-52.

3. Radziemska E The impact of temp on the control drop in crystalline sun powered cells[J].Renewable Energy. 2003,28(1):1-12 .

4. Klugmann E .Impact of temp on change proficiency of a sun powered module working in photovoltaic PV/T coordinates system[C]//16th European photovoltaic solar vitality conference,Glasgow,UK,200 .

5. Hegazy A A. Comparative consider of the exhibitions of four photovoltaic/ thermal sunpowered discuss collectors[J].Energy Transformation and Ad ministration,2000,41(8):86l-881 .

6. He W ,Chow T T ,Li J,et al.Hybrid photovoltaic and thermal solar–collector designed for natural circulation of water[J].Applied Energy,2006,83(3):199-210 .

7. Chow T T ,He W ,Li J . cross breed photovoltaic thermos siphon water heating framework for private application [J].Solar Energy,2006,80 (3):298-306 .

8. Li M,Ji X,Li G L.et al. Execution examination and optimization of the Trough Concentrating Photovoltaic/ Thermal system[J].Solar Energy ,2011 ,85(5) :1028-1034.

9. Russell M C, Kern E C , .Combined photovoltaic and thermal cross breed collector systems[C]//Proceeding of the 13th IEEE Photovoltaic pros,Washington DC , USA,1978 .

10. Chow T T .An audit on photovoltaic/thermal crossover solar technology[J]. Applied Energy,2010,87(2):365-379 .

11. Zondag H A. Flat-plate PV-Thermal collector and framework : an audit [J].Renewable and Sustainable Energy Review,2008,12(4):891-959 .

12. Joshi A S,Dincer I,Reddy B V. Execution investigation of photovoltaic systems: an audit [J] .Renewable and Sustainable Energy Reviews,2009,13(8):1884-1897 .

13. Hasan M A,Sumathy K. Photovoltaic thermal module concepts and their execution examination :an audit [J] .Renewable and Sustainable Energy Reviews,2010,14(7):1845-1859.

14. Charalambous P G,Maidment G G,Kalogirou S A,et al. Photovoltaic thermal (PV/T) collectors : an audit [J].Applied Thermal Engineeri ng,2007,27(2-3):275-286

15. Wang Baoqun,Yao Qiang,Song Qiang,et al. Photovoltaic-thermal

(PV/T) frameworks and their evaluation[J].Acta Energiae Solaris Sinica ,2009 ,30(2): 193-200

16. Lu Zhiheng ,Yao Qiang. Level plate sun powered vitality photovoltaic thermal (PV/T) combined panel[J].Energiae Solaris Sinica,2006,27(6):545-552

17. Wang Yiping,Liu Yonghui,Tianwei. Investigate advance on crossover PV/thermal sun powered system[J].Energiae Solaris Sinica,2005,26(5):639-646

18. Pei Gang ,Fu Huide,Zhang Tao,et al. A numerical and exploratory think about on a heat pipe PV/T system[J].Solar Energy,2011,85(5):911-921 .

19. Skoplaki E,Palyvos J A. On the temp reliance of photovoltaic module electrical execution : an audit of efficiency/power correlations[J].Solar Energy,2009,83(5):614-624 .

20. Zhang, Yang ,Zhuang.Energy-saving innovation of heat pipe[M]. Chemical Industry Press,Chinese,1976,36.

21. Hussein H M S. Hypothetical and exploratory examination of wickless heat channels level plate sun based collector with cross stream heat exchanger[J]. Energy Conversion and Management,2007,48(4):1266-1272 .

22. Arvind T,Sodha M S. Execution assessment of solar PV/T framework: an exploratory validation[J].Solar Energy,2006,80(7):751-759 .